

# Grid Assessment Using the NASA Common Research Model (CRM) Wind Tunnel Data

Leonardo C. Scalabrin\* and Rodrigo F. de Souza†

*EMBRAER S.A., Sao Jose dos Campos - SP - Brazil.*

A commercial Computational Fluid Dynamics (CFD) code is used to simulate transonic flow conditions over the NASA Common Research Model. The results are obtained using the unstructured set of grids available from the 5th Drag Prediction Workshop and several unstructured custom grids generated at EMBRAER. A grid convergence study is performed for different sets of grids: hexahedral, triangular based prisms and hybrid meshes. Comparisons of drag, pitching moment and pressure distributions are presented. The industry established SST and SA turbulence models are used to simulate the flow. Results are compared to available wind tunnel data for forces, moments and pressure distributions.

## I. Introduction

ACCURATE drag prediction is a fundamental part in the design of any aircraft. In the past few years, with the rising uncertainties in oil prices and the environmental pressure for more efficient vehicles, performance differences of less than one percent can determine the economical feasibility of a new commercial aircraft design.

One of the available tools for drag prediction is Computational Fluid Dynamics (CFD).<sup>1</sup> The improvements in algorithms and computer power enabled CFD to become an important part of the design process. However, it was recognized in the CFD community that the numerical results presented large variations depending on the numerical scheme employed, the grids used and the user performing the analysis. Such variations can become an issue during aircraft design, where comparisons of geometry performance are routinely performed. The results of flow simulations over different geometries need to be consistent to allow a meaningful comparison. In order to achieve this consistency, variations in the flow solution due to grid, scheme and user input need to be avoided.

In order to better study the variations due to grid, scheme and user input, a series of drag prediction workshops promoted by AIAA<sup>2-5</sup> were performed. Every workshop was a chance to reduce the spread between the drag predictions and a forum to discuss methodologies and limitations of the available numerical codes. The 5th Drag Prediction Workshop was held during the 42nd AIAA Fluid Dynamics conference, in New Orleans in 2012. This workshop differed from the others because it provided a common set of grids<sup>6-8</sup> that could be used by almost any CFD code, greatly reducing grid dependence from the comparisons.

The objective of this paper is to document the results EMBRAER obtained as part of its DPW-5 participation using a commercial CFD solver. A grid convergence study is performed for the provided DPW-5 grids and also for custom grids generated at EMBRAER. The DPW-5 grids are made of hexahedral, triangular based prisms and tetrahedra (hybrid) meshes while the custom grids are composed of tetrahedra and layers of triangular base prisms at the body. Two different turbulence models are used in the simulations to evaluate its impact on the solutions: the industry established SA<sup>13-15</sup> and SST<sup>16</sup> turbulence models. Those simulations are focused on comparisons with wind tunnel coefficients and pressure distribution.

## II. Modeling

The transonic flow is modeled using the Reynolds Averaged Navier-Stokes equations (RANS) with turbulence model closures.<sup>1</sup> Air is modeled as a perfect gas, with viscosity calculated using Sutherland's law. The

\*Product Design Engineer, Advanced Design, AIAA Member.

†Product Design Engineer, Advanced Design, AIAA Member.

equations are solved numerically using the commercial software CFD++ available at EMBRAER. CFD++ is a finite-volume code, that models the inviscid terms using upwind fluxes and reconstruction algorithms<sup>9–11</sup> for higher spatial order of accuracy. The time march is performed using a point-implicit method and using multigrid for convergence acceleration. CFD++ has a wide range of turbulence models implemented. In this work, the aerospace industry established models SST<sup>16</sup> and SA<sup>13–15</sup> are employed. The boundary conditions used are adiabatic walls for the aircraft, characteristic based relations for the farfield and symmetry for the symmetry plane.

## II.A. Grids

Several sets of grids are employed in this study. The grids used for the DPW-5 workshop are listed in table 1. Some were provided by the DPW-5 committee and are labelled “Common” grids. The grids generated internally at EMBRAER for the workshop are labelled “Custom”. EMBRAER grids are generated using the commercial softwares ICEMCFD for the surface grid (made of triangles) and TGRID for the volumetric grids (made of triangular base prisms and tetrahedra). The grids are also compared visually in Figs. 1, 2 and 3 according to their refinement level (2: coarse, 3: medium and 4: fine).

**Table 1. Grids used in the DPW-5 workshop**

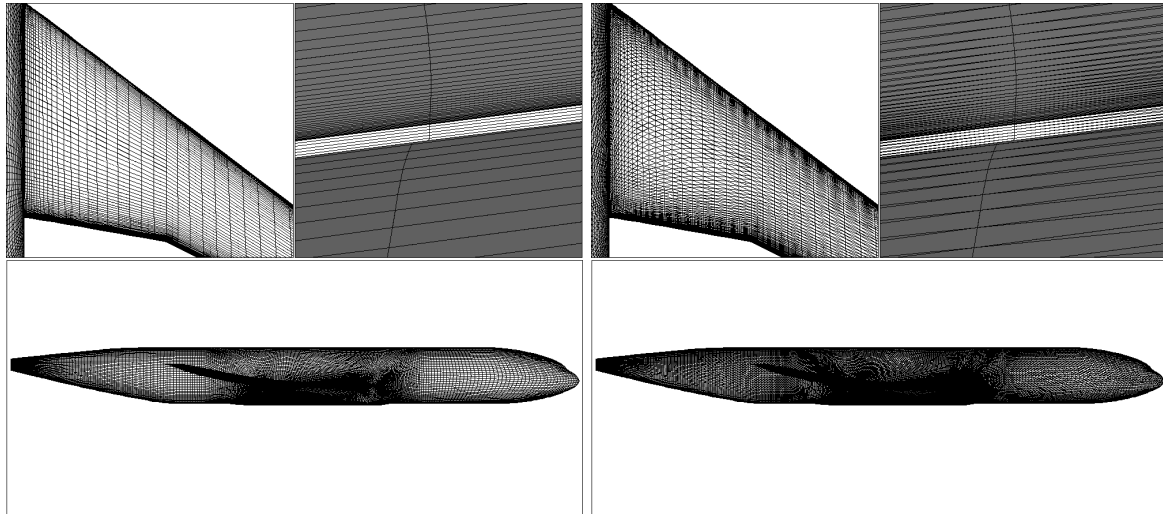
Grid ID	Origin	Element types	Refinement Level	Number of Cells
CommonHex	DPW-5	Hexa	2	2156544
CommonHex	DPW-5	Hexa	3	5111808
CommonHex	DPW-5	Hexa	4	17252352
CommonHybrid	DPW-5	Tetra	2	10063872
CommonHybrid	DPW-5	Tetra	3	24068096
CommonHybrid	DPW-5	Tetra	4	80990208
CommonPrism	DPW-5	Prisms	2	4313088
CommonPrism	DPW-5	Prisms	3	10223616
CommonPrism	DPW-5	Prisms	4	34504704
CustomHybrid	EMBRAER	Prisms and tetra	2	7105882
CustomHybrid	EMBRAER	Prisms and tetra	3	15535198
CustomHybrid	EMBRAER	Prisms and tetra	4	20627935

It is important to notice that the Common set of grids are based on the CommonHex grid. Even the CommonHybrid and the CommonPrism are generated from the splitting of the hexahedra in the CommonHex into tetrahedra and triangular base prisms. This procedure generates unstructured grids that have faces distributed similarly to a hexa grid i.e. approximately aligned to the flow direction. It is expected that this may improve gradient calculations and consequently lead to better solutions.

The Custom grid, on the other hand, is a trully unstructured grid. The nodes and faces of the tetrahedra are distributed randomly, except at the prism layer which presents some regularity which is fundamental to capture the strong gradients in the boundary layer. The Custom grid do not have a very refined wing trailing edge because it created difficulties for prism generation.

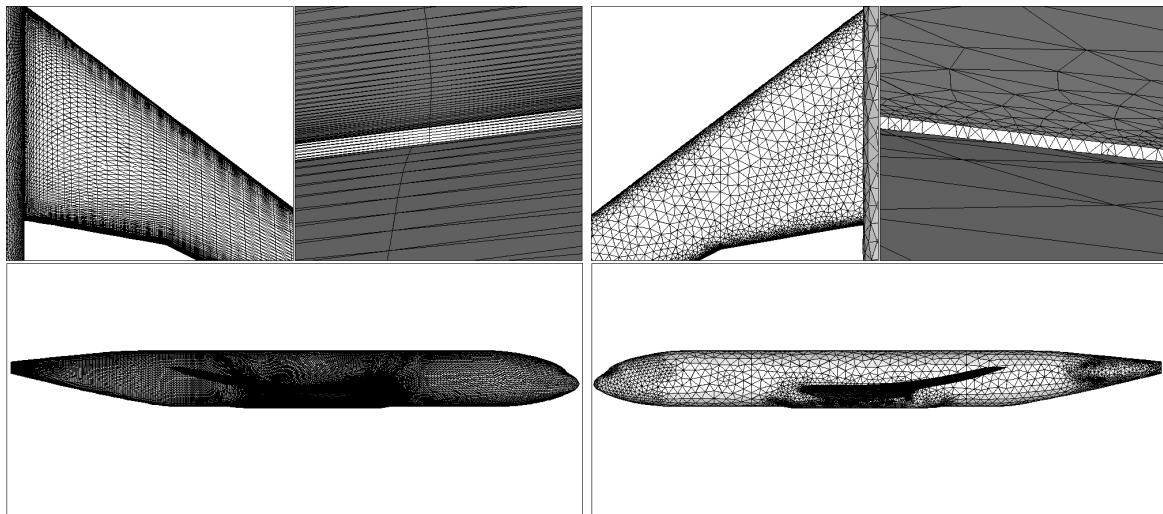
From the Figs. 1, 2 and 3, it became clear that the grids generated at EMBRAER do not present the same regular distribution of points as the Common set of grids. New grids were generated as an attempt to assess the dependence of the results in relation to the refinement in some areas of the grid. Four sets of custom grids were generated in addition to the custom grid used for the DPW-5 workshop. They are listed in Tab. 2.

The areas for additional grid refinement are the fuselage and the wing. The Custom grids CustomHybridM1 and CustomHybridM3 are depicted in Fig. 4. CustomHybridM1 has the same surface refinement at the fuselage as the grid CustomHybrid but a more refined surface grid on the wing. CustomHybridM3 has the same surface refinement at the wing as the grid CustomHybrid but a more refined surface grid on the fuselage. Grid CustomHybridM9 has the same surface grid as M1 but with refinement boxes over the wing to provide better refinement outside the prism layer, as can be seen in Fig. 5, mainly to improve the shock wave resolution.



(a) CommonHex

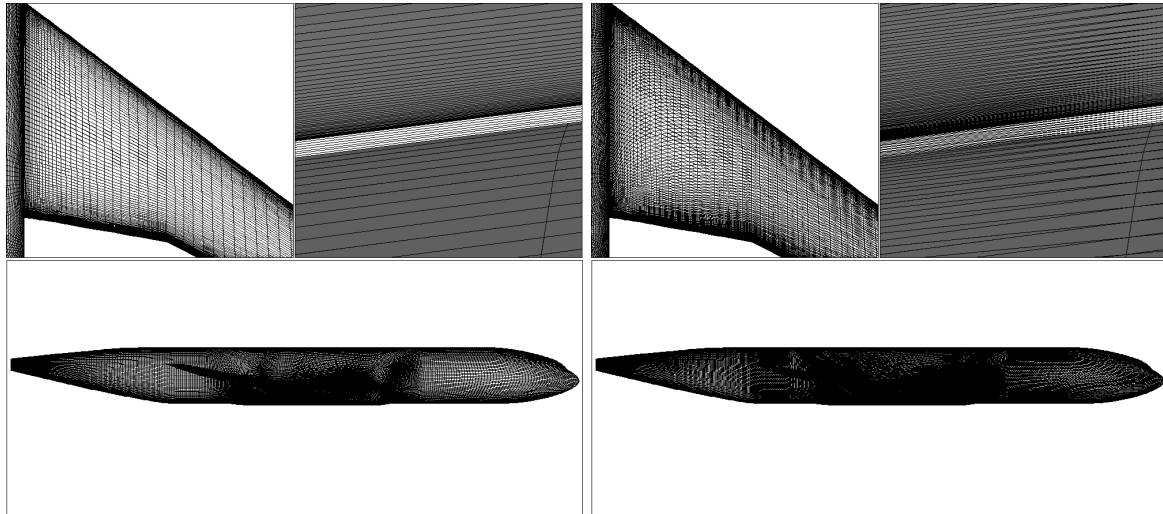
(b) CommonHybrid



(c) CommonPrism

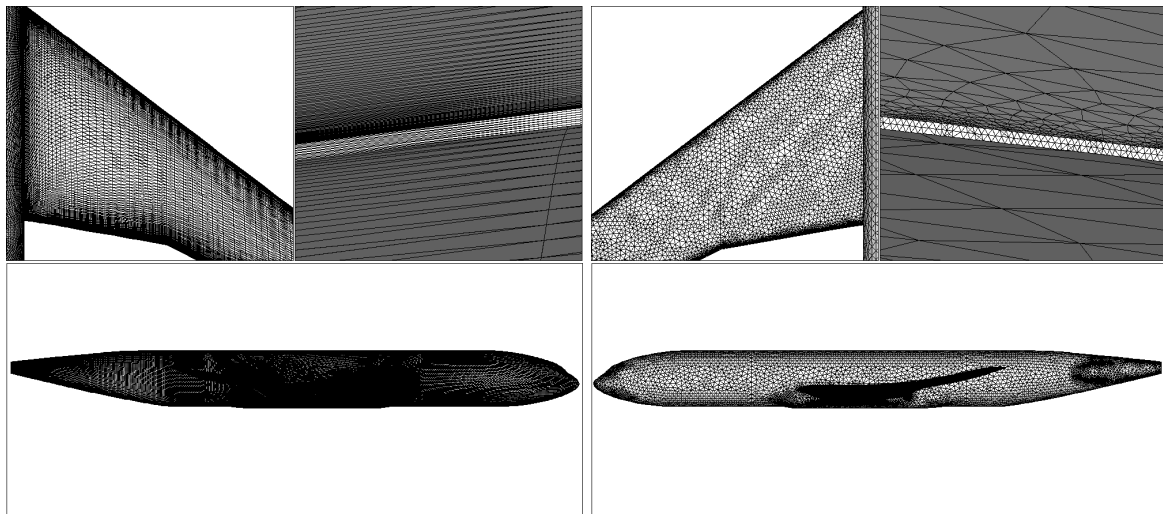
(d) CustomHybrid

Figure 1. Grid topology and refinement comparison - Coarse



(a) CommonHex

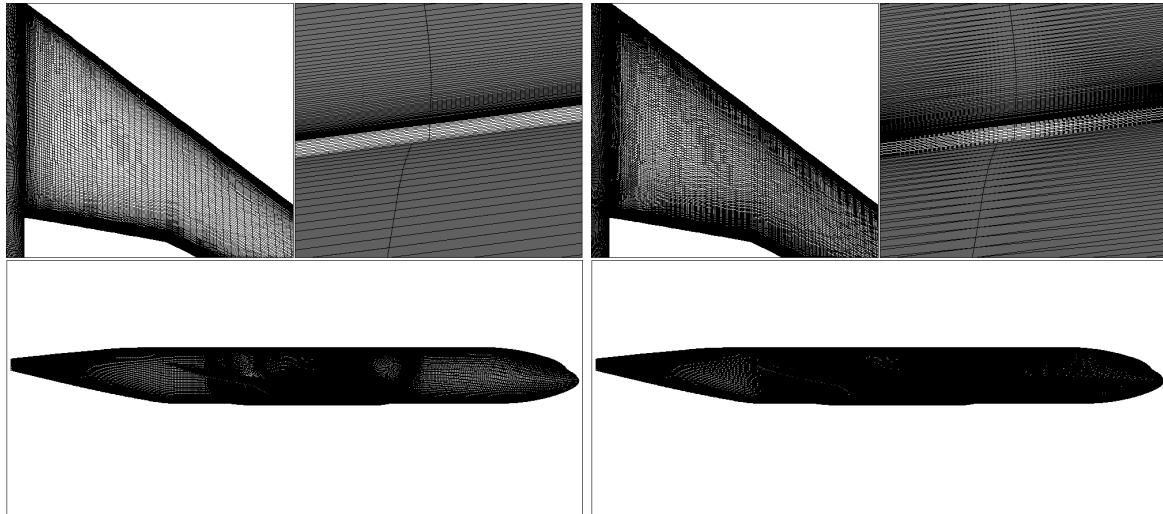
(b) CommonHybrid



(c) CommonPrism

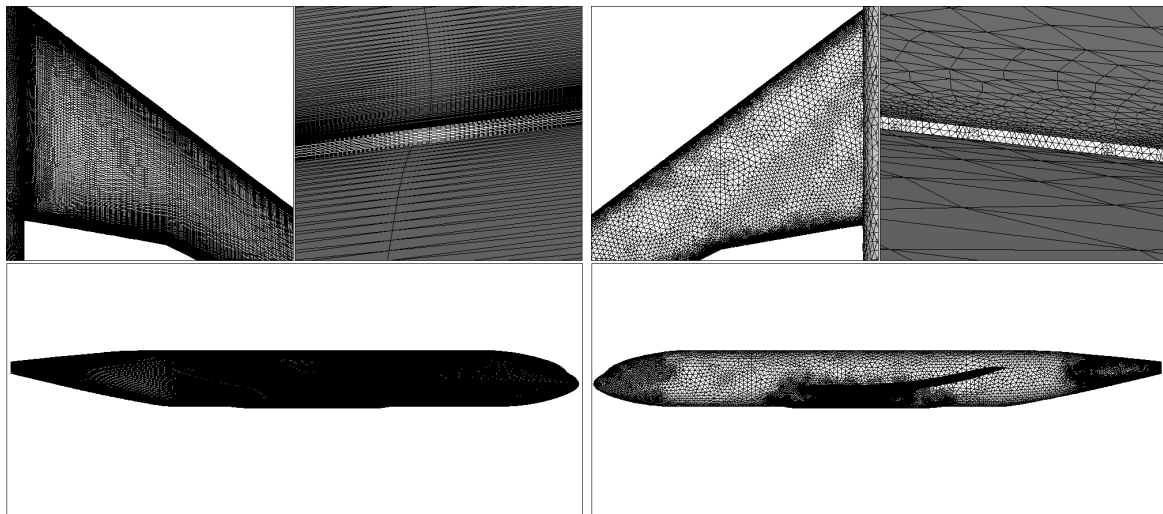
(d) CustomHybrid

**Figure 2. Grid topology and refinement comparison - Medium**



(a) CommonHex

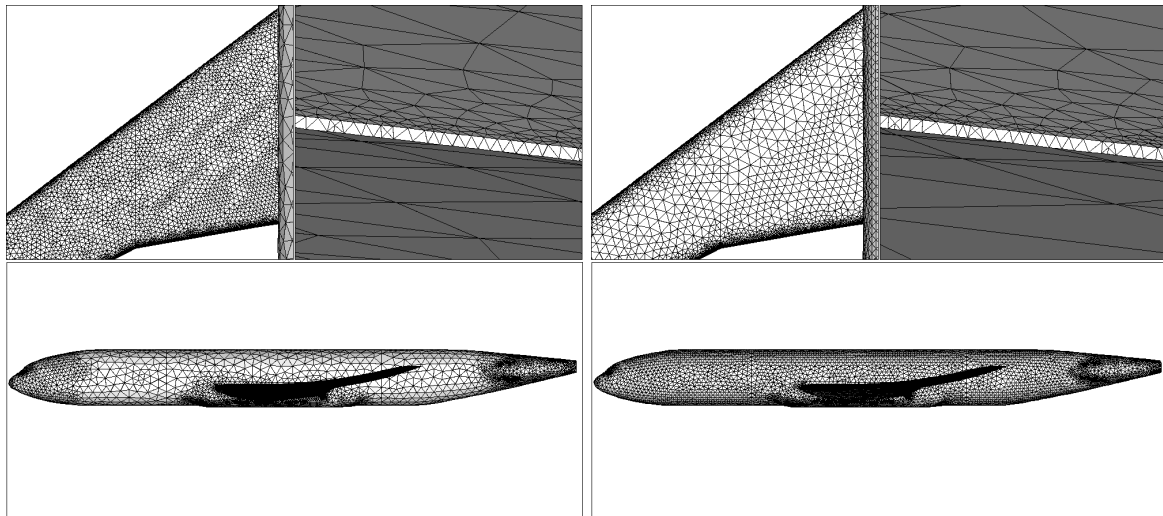
(b) CommonHybrid



(c) CommonPrism

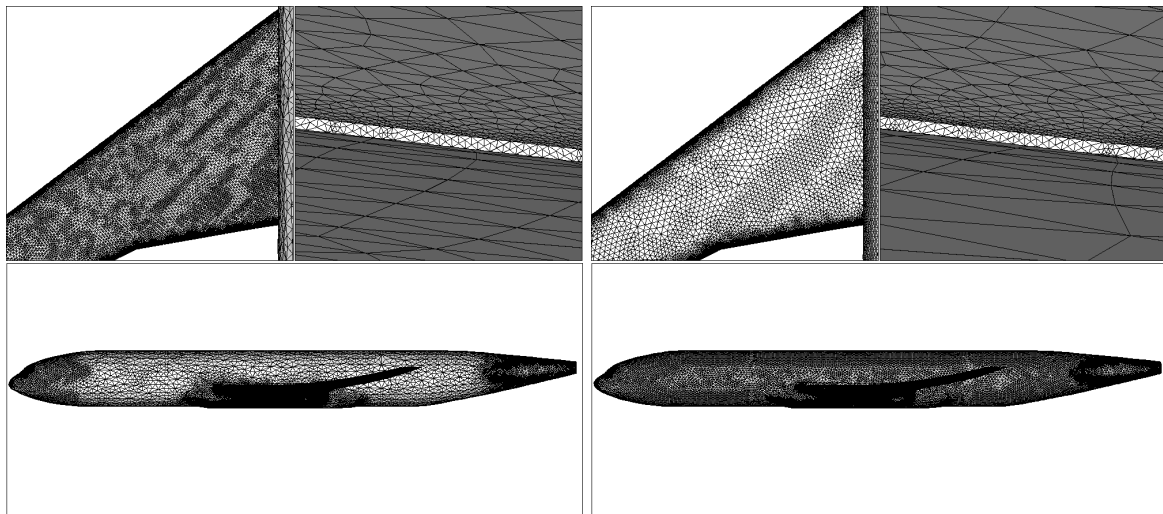
(d) CustomHybrid

**Figure 3. Grid topology and refinement comparison - Fine**



(a) CustomHybridM1 - Coarse

(b) CustomHybridM3 - Coarse



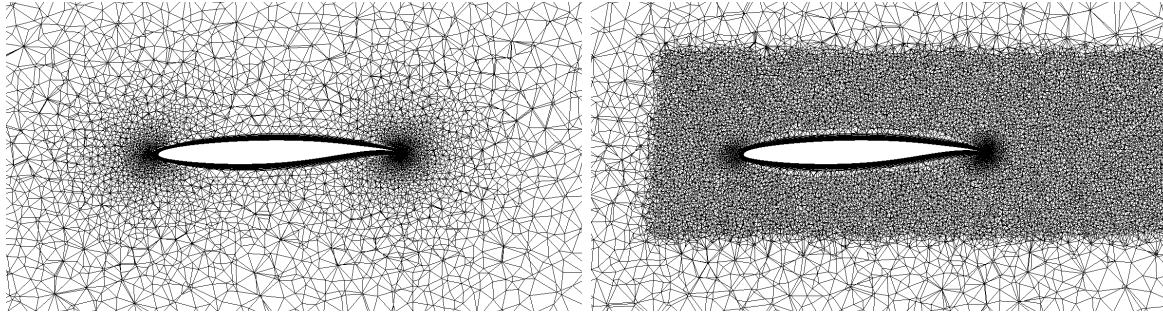
(c) CustomHybridM1 - Medium

(d) CustomHybridM3 - Medium

**Figure 4. Grid topology and refinement comparison - Grids CustomHybridM1 and CustomHybridM3**

Table 2. Additional Custom Grids

Grid ID	Origin	Element types	Refinement Level	Number of Cells	Refinement area
CustomHybridM1	EMBRAER	Prisms and tetra	2	7534081	Wing
CustomHybridM1	EMBRAER	Prisms and tetra	3	18092329	Wing
CustomHybridM3	EMBRAER	Prisms and tetra	2	7318952	Fuselage
CustomHybridM3	EMBRAER	Prisms and tetra	3	17510114	Fuselage
CustomHybridM9	EMBRAER	Prisms and tetra	2	10234709	Wing and volume
CustomHybridM9	EMBRAER	Prisms and tetra	3	30245316	Wing and volume



(a) CustomHybridM1 - Medium

(b) CustomHybridM9 - Medium

Figure 5. Volumetric refinement comparison - Grids CustomHybridM1 and CustomHybridM9

### III. Results

A Cluster of Xeon 5690 processors was used for the simulations. The conditions for the simulations are shown in Table 3. It consists of two different studies: a grid refinement and a buffeting study.

Table 3. Flow conditions for the simulations

Study	Alpha	CL	Mach	Re
Grid refinement	-	0.50	0.85	5 millions
Buffeting	2.5, 2.75, 3.0, 3.25, 3.5, 3.75, 4.0	-	0.85	5 millions

The grid refinement case is used to assess the dependence of the drag coefficient due to grid variations, while the buffeting study is used to evaluate the behavior of the CFD solutions when some flow separation is present.

#### III.A. Grid Refinement Study

Figure 6(a) presents the grid dependence for the CRM model total drag. It can be observed that both the CommonHex and the CommonPrism grids have less grid refinement dependence than the CommonHybrid and CustomHybrid grids.

The CommonHybrid results raised some concern, because other CFD++ users at the DPW-5 workshop were able to obtain better results with that grid. A different setting in the CFD++ solver was used in order to improve the results. This new setting uses a more accurate way to calculate gradients in grids of tetrahedra. It uses node based polynomials instead of cell center based polynomials. A comparison of results obtained using both methods is shown in Fig. 6(b). It can be observed that the use of nodal polynomials reduces significantly the grid refinement dependence for the CommonHybrid grids. This may be explained because the CommonHybrid grid shares the node positions with the CommonHex grid. In this case, CFD++'s

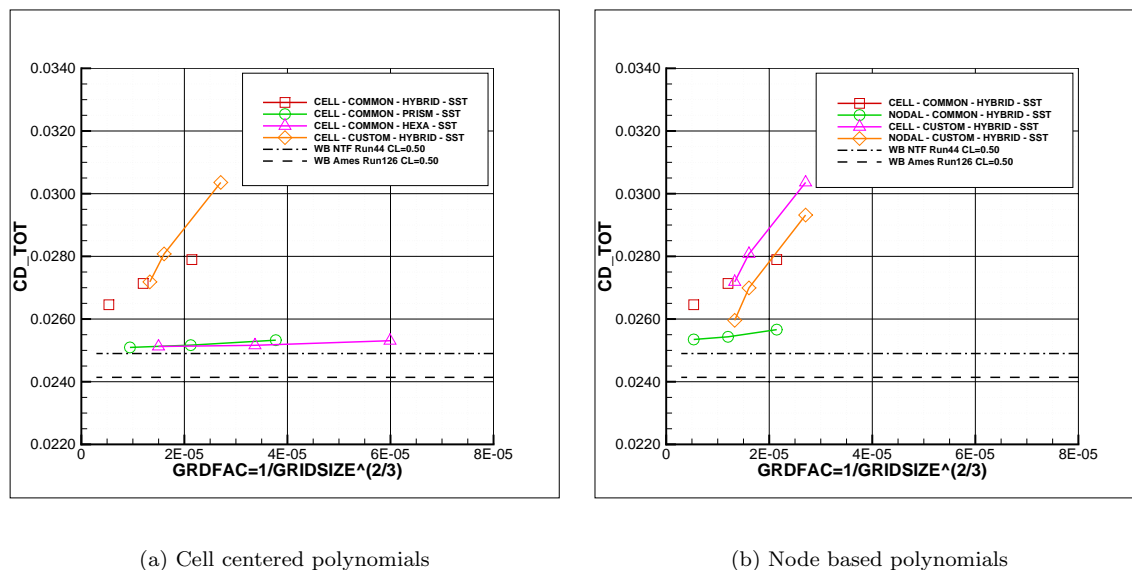


Figure 6. Grid convergence for the CRM model total drag at  $M=0.85$ ,  $Re=5$  millions and  $CL=0.50$ .

nodal polynomials are able to recover a grid refinement dependence similar to that of the CommonHex and CommonPrism grids. However, this was not achieved with the CustomHybrid grids, a truly unstructured grid. In this case, the nodal based polynomials offered an improvement in drag levels but it did not reduce the dependence of the result in relation to grid refinement.

Further investigation shows that the grid refinement dependence in the Custom-hybrid mesh is caused mostly by the pressure part of the drag as can be observed in Figs. 7(a) and 7(b). If the skin friction is not very dependent on the grid, the grid refinement dependence may be caused by the surface grid on the CRM model. In addition, the fuselage and wing drag were separated to verify if the grid dependence was limited to a particular region of the aircraft. The results are shown in Figs. 8(a) and 8(b). It can be observed that the grid dependence is more strongly related to the wing refinement but the refinement on the fuselage also causes grid dependence. All these observations triggered improvements in the CustomHybrid grids and the generation of the additional custom grids CustomHybridM1, CustomHybridM3 and CustomHybridM9.

The results obtained using the additional custom grids are shown in Fig. 9. It shows that the additional custom grids have similar behavior to the original Custom grid. The surface grid refinement on the fuselage (CustomHybridM3) improves the fuselage drag as expected, but the surface refinement on the wing (CustomHybridM1) had no significant impact on wing drag, as can be observed in Fig. 10. The grid CustomHybridM1 has much more surface grid refinement on the wing. Figure 10(b) seems to indicate that surface grid refinement alone is not enough to accurately capture the wing drag contribution to total drag. The addition of volume refinement on grid CustomHybridM9 also did not improve the results of wing drag obtained by the grids CustomHybridM1 and CustomHybridM3. This result may suggest that the alignment of grid faces to the flow direction is important, something that cannot be easily obtained using a truly unstructured grid generator.

### III.B. Buffeting studies

The lift divergence, one of the criterias to predict the buffet onset, can be determined using the  $CL \times \alpha$  and  $CL \times CM$  curves. They are shown in Fig. 11 for different types of grid. It can be observed that the CustomHybrid grid clearly detaches from the other solutions and also presents an anticipation of the lift divergence. This anticipation indicates excess of flow separation for the same lift coefficient, which may be related to an excess of artificial dissipation introduced by the truly unstructured grid.

The solutions obtained using the other grids are very similar for  $\alpha = 2.5$  degrees. The gap between the solutions increases with angle-of-attack, a sign that even flow solutions using the same CFD code and the

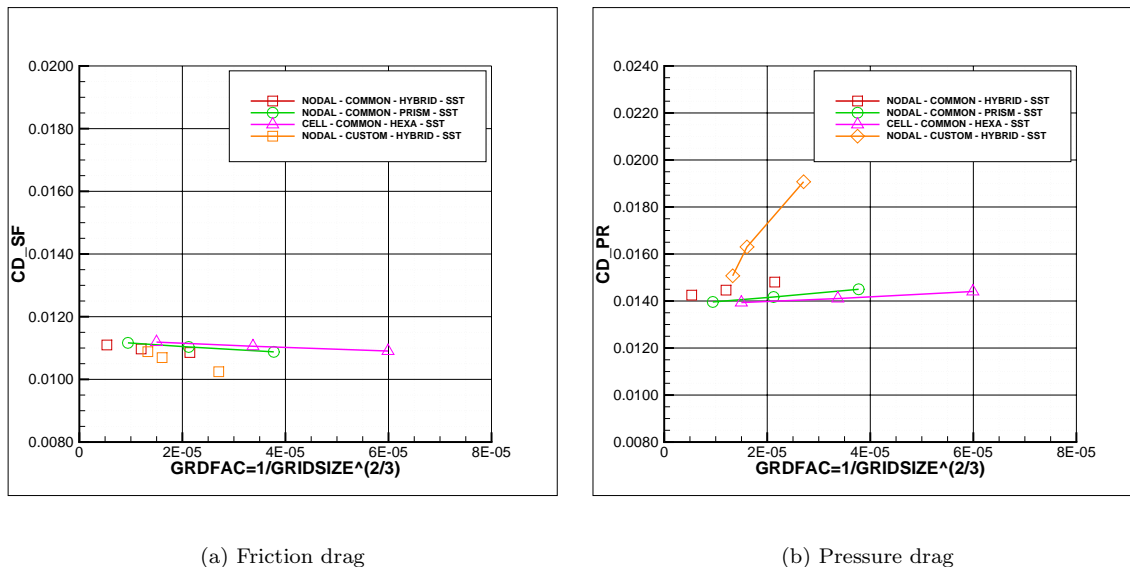


Figure 7. Grid convergence for the CRM model friction and pressure drag at  $M=0.85$ ,  $Re=5$  millions and  $CL=0.50$ .

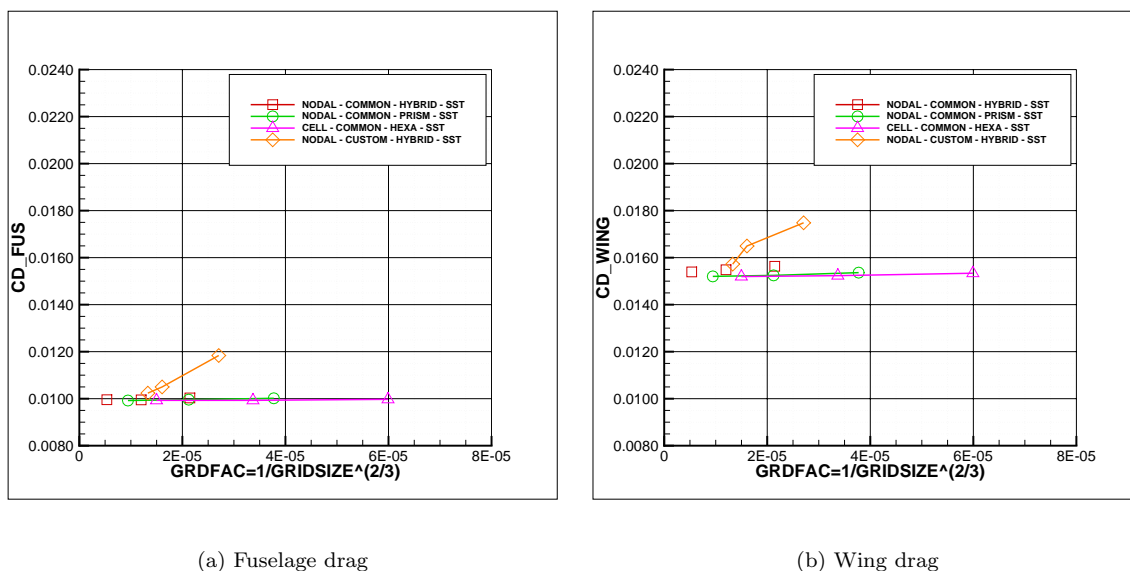


Figure 8. Grid convergence for the CRM model fuselage and wing drag at  $M=0.85$ ,  $Re=5$  millions and  $CL=0.50$ .

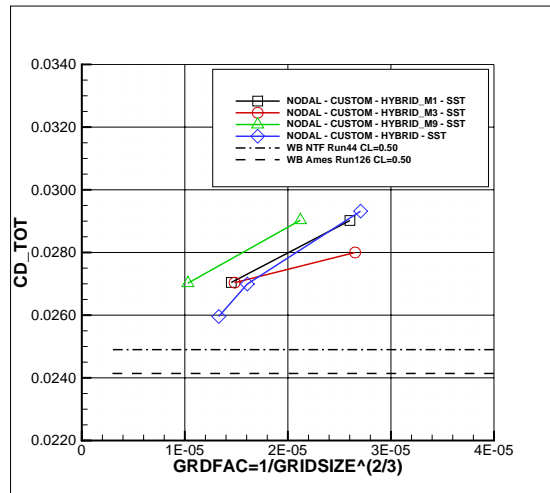
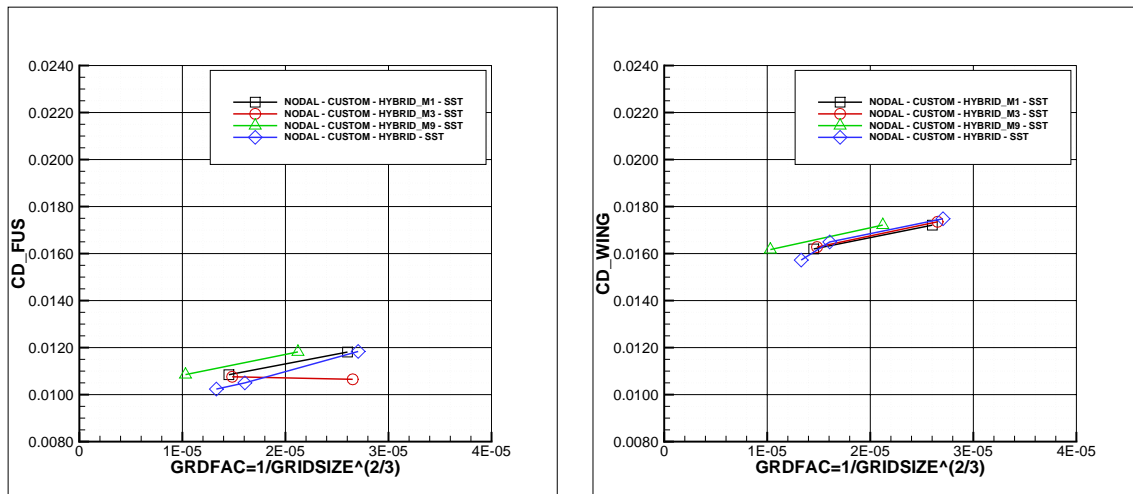


Figure 9. Grid convergence for the CRM model total drag at M=0.85, Re=5 millions and CL=0.50 with the Custom grids.



(a) Fuselage drag

(b) Wing drag

Figure 10. Grid convergence for the CRM model fuselage and wing drag at M=0.85, Re=5 millions and CL=0.50.

same turbulence model are very dependent on the type of grid (hexa, prism or tetra). The same behavior can be observed in Fig. 12. The solution obtained using the custom grid is clearly off the other solutions, indicating it needs improvements. The common set of grids provided by DPW-5 show the great impact of mesh type in the solution obtained by a CFD code when the flow starts to exhibit separation.

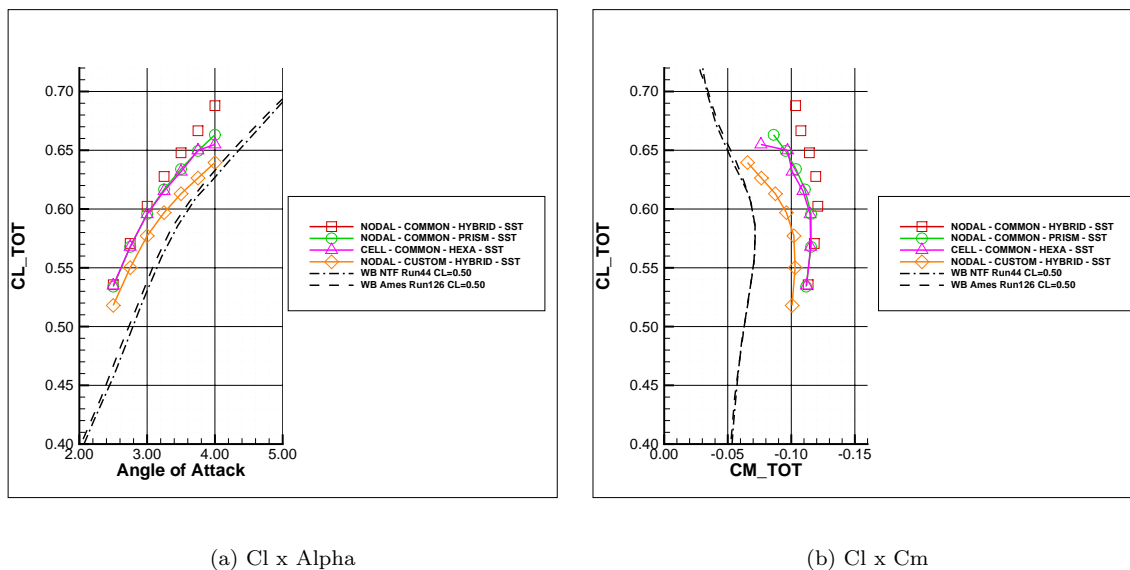


Figure 11. Buffeting study,  $M=0.85$ ,  $Re=5$  millions and  $CL=0.50$ .

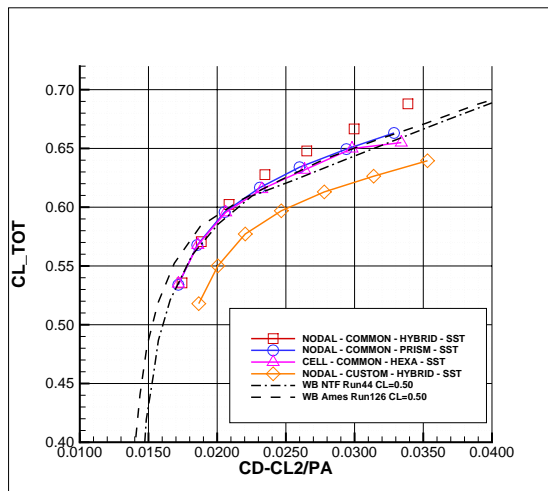


Figure 12.  $Cl \times Cd$  curve,  $M=0.85$ ,  $Re=5$  millions and  $CL=0.50$ .

Figures 13 to 16 present comparisons between the pressure distribution at wing stations 4, 6, 9, 10, 12 and 14 for angles-of-attack 2.50, 3.25, 3.75 and 4.00 degrees. It can be observed that for  $\alpha = 2.50$  degrees, the pressure distribution at all stations agree very well between the 3 types of grids. It should be noted that the custom grid was removed from the comparisons due to its poor characteristics for the  $CL \times \alpha$ ,  $CL \times C_m$  and  $CL \times C_d$ . Differences in the pressure distribution due to the grid start to appear as the angle-of-attack increases. The differences are more visible at stations 10 and 12. The differences are mainly the shock position, which is more aft when using the CommonHybrid grid, and the trailing edge separation. At station 10, the solutions using the CommonHex and CommonPrism are similar and the CommonHybrid stand out. At station 12, the pressure distribution is different between the grids.

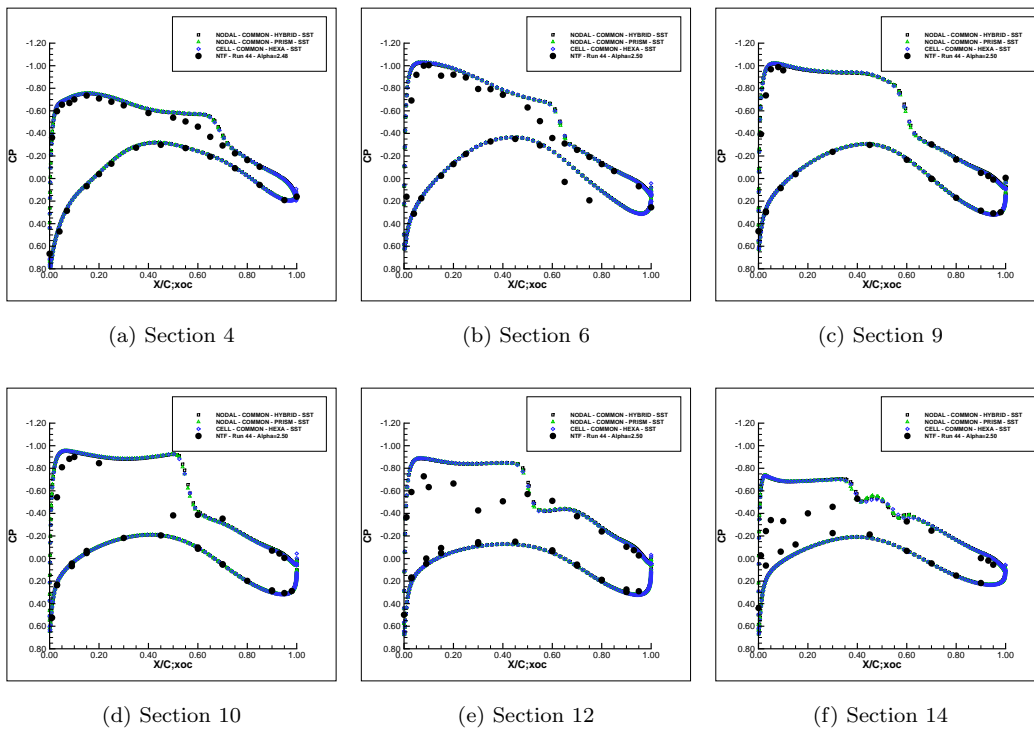


Figure 13. Pressure coefficient distributions,  $M=0.85$ ,  $Re=5$  millions and  $\text{Alpha}=2.50$

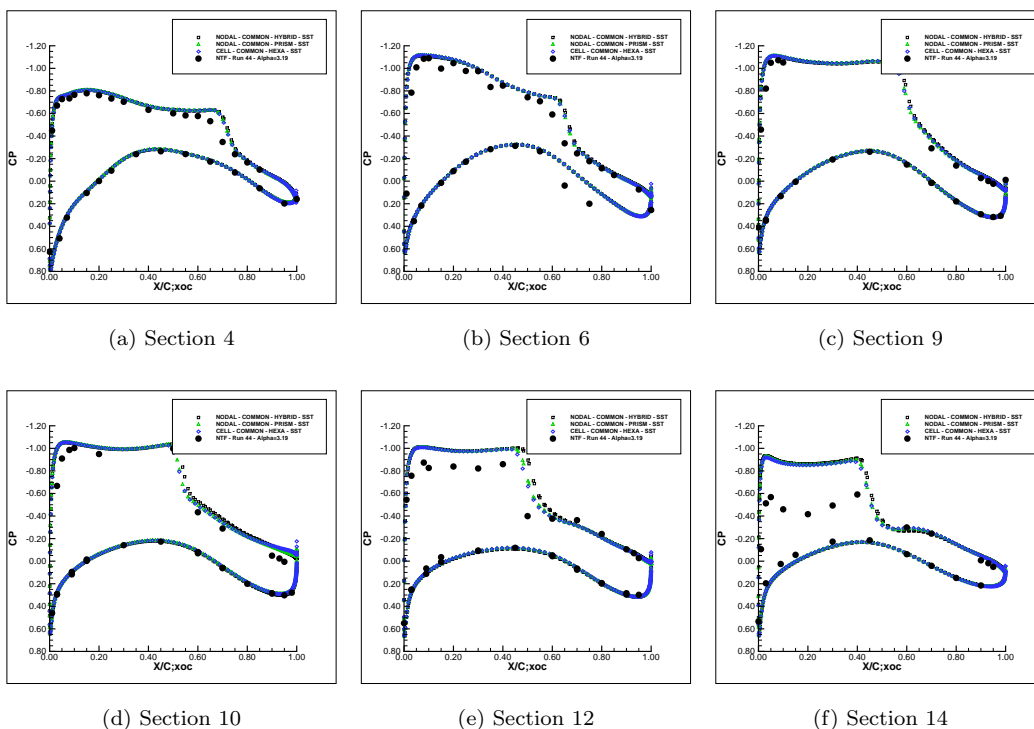


Figure 14. Pressure coefficient distributions,  $M=0.85$ ,  $Re=5$  millions and  $\text{Alpha}=3.25$

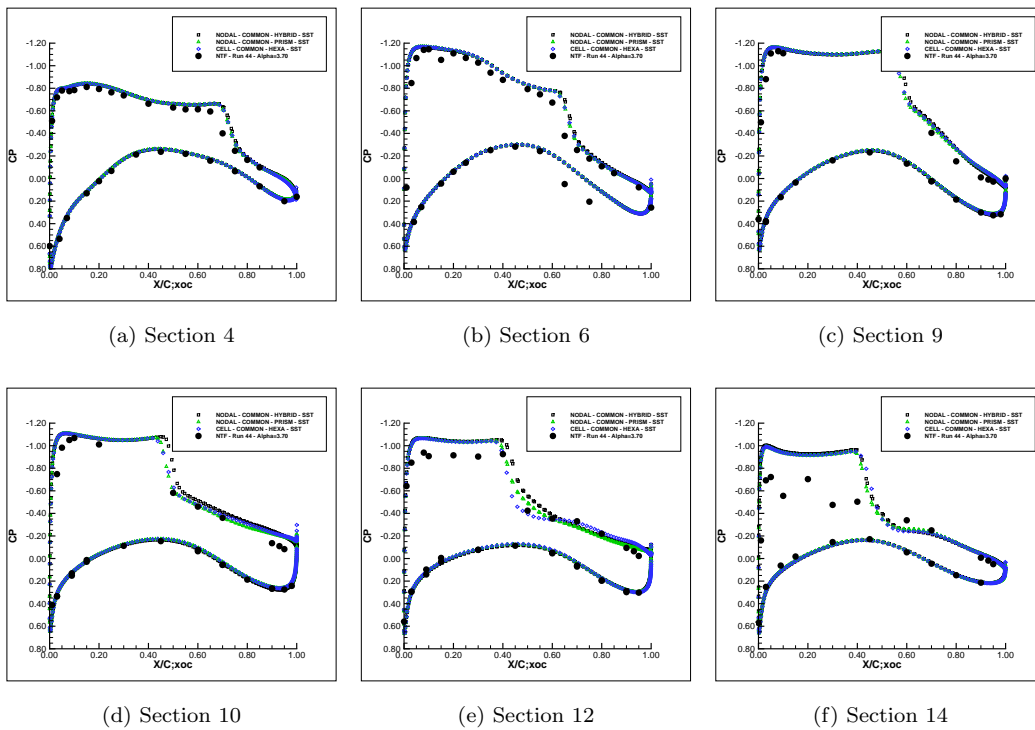


Figure 15. Pressure coefficient distributions,  $M=0.85$ ,  $Re=5$  millions and  $\text{Alpha}=3.75$

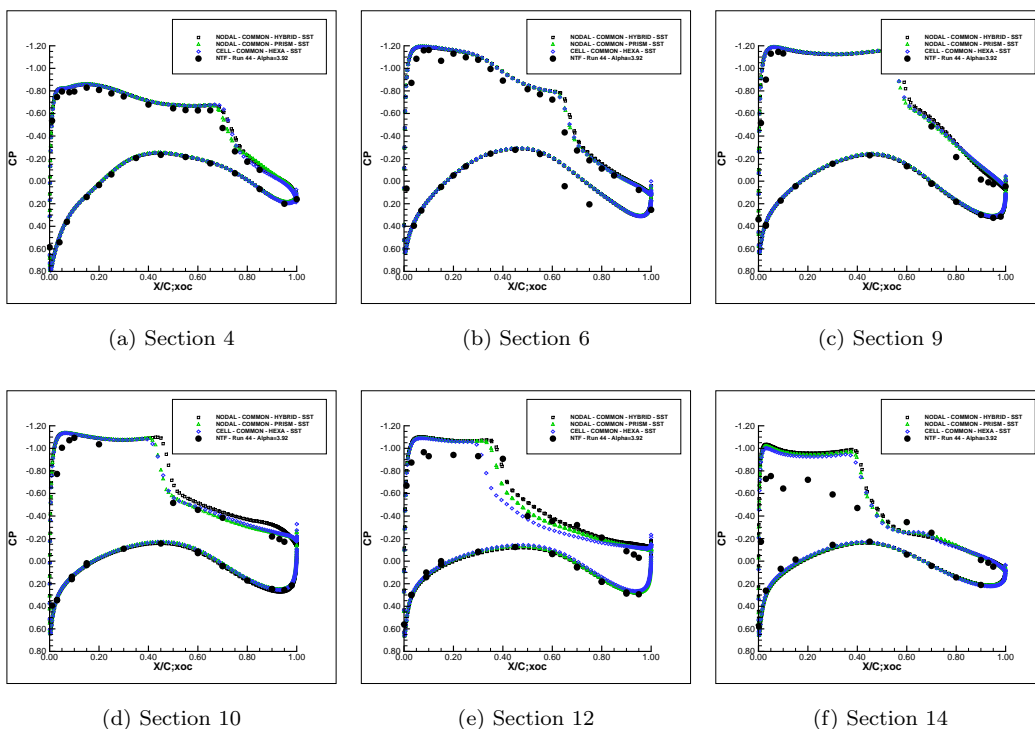


Figure 16. Pressure coefficient distributions,  $M=0.85$ ,  $Re=5$  millions and  $\text{Alpha}=4.00$

### III.C. Turbulence model studies

Figure 17 presents a comparison of the total drag calculated using the SST and the SA turbulence models. It can be observed that for both grids, the drag calculated using the SST model is consistently below the value calculated using the SA model.

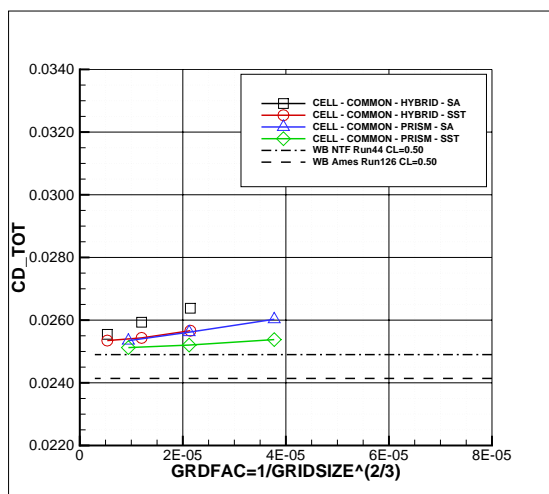
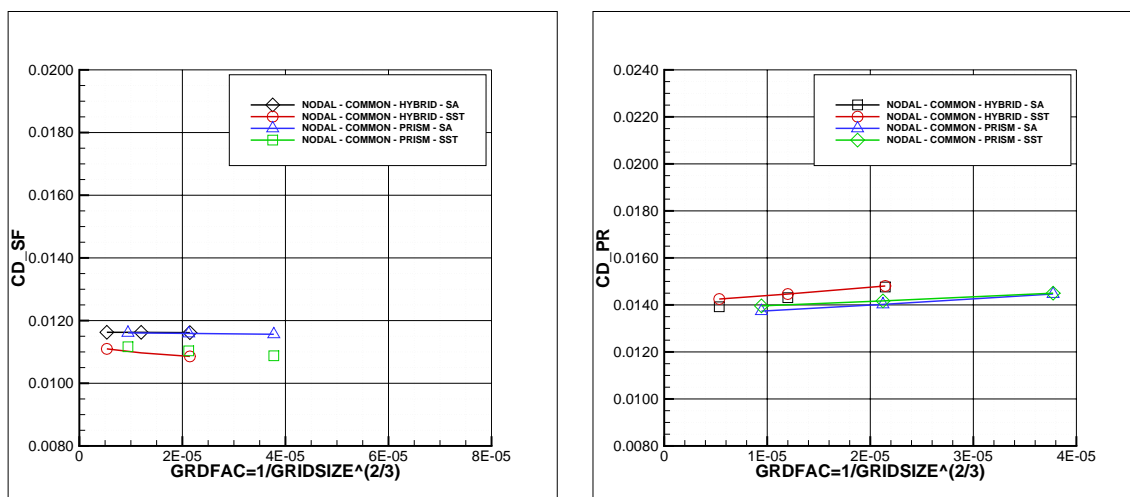


Figure 17. Total drag,  $M=0.85$ ,  $Re=5$  millions and  $CL=0.50$ .

Such behavior is explored in terms of friction and pressure drag in Fig. 18. The difference is mostly related to the friction drag which is smaller when using the SST model, an expected characteristic. The pressure drag values are very similar for both models. This fact is also corroborated by the pressure distributions in stations 4, 6, 9, 10, 12 and 14, which are shown in Fig. 19. The differences between the pressure distributions calculated using both models for the CommonPrism mesh are barely noticeable.



(a) Friction drag

(b) Pressure drag

Figure 18. Grid convergence for the CRM model friction and pressure drag at  $M=0.85$ ,  $Re=5$  millions and  $CL=0.50$ .

A comparison of  $CL\alpha$  curves is presented in Fig. 20. The lift curve calculated using the SST turbulence model is also consistently below the lift curve obtained using the SA model. Figures 21 and 22 are used in order to visualize the causes for such behavior. It is observed that the pressure distribution with the SA model presents a more aft shock. This is more clearly seen at station 10 for  $\alpha = 4.00$ , which also shows that the SA model has a lower pressure after the shock which also creates more lift.

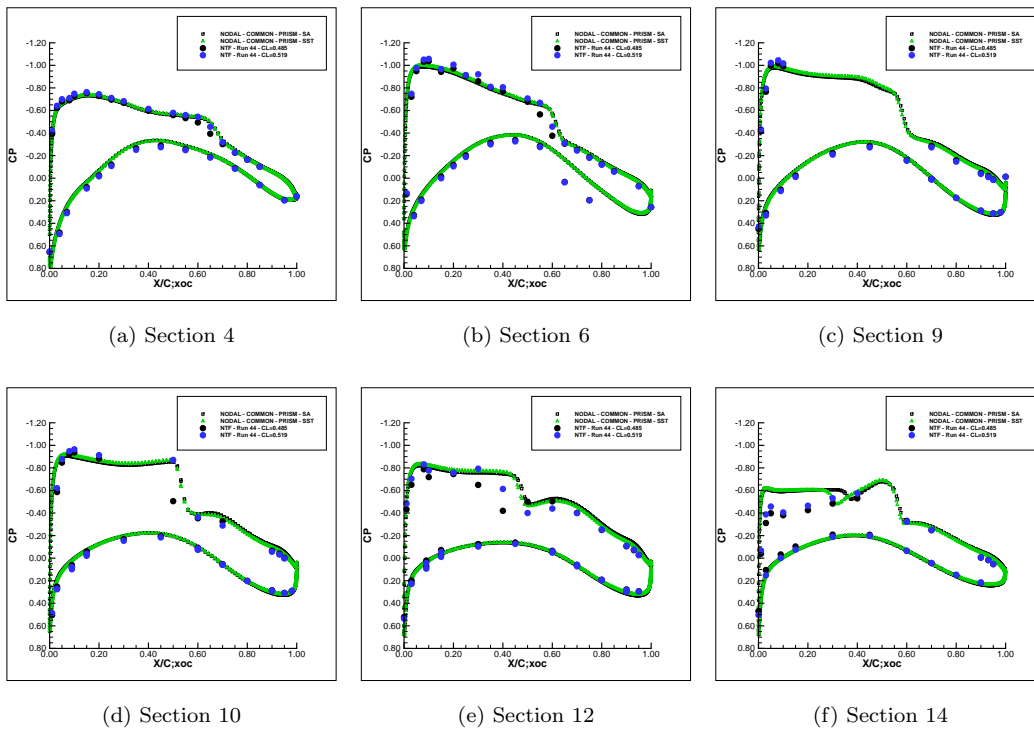


Figure 19. Pressure coefficient distributions,  $M=0.85$ ,  $Re=5$  millions and  $CL=0.50$

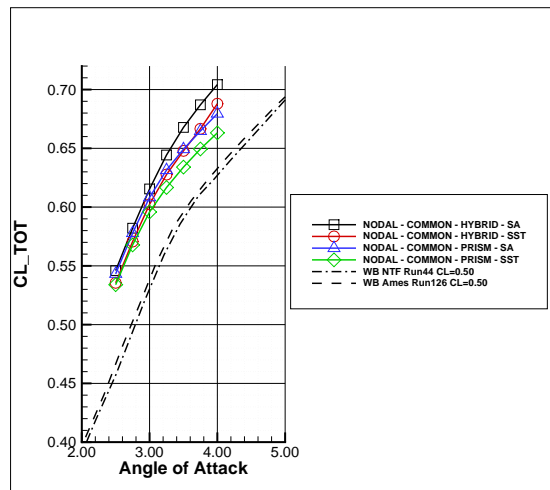


Figure 20.  $Cl_x\alpha$ ,  $M=0.85$ ,  $Re=5$  millions

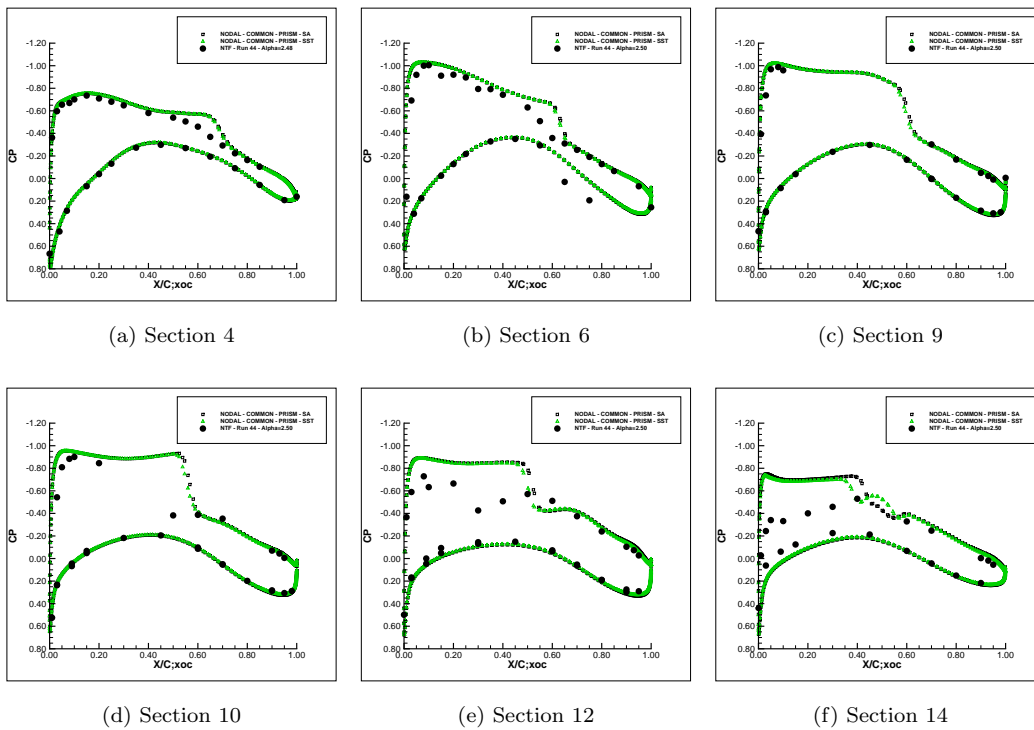


Figure 21. Pressure coefficient distributions,  $M=0.85$ ,  $Re=5$  millions and  $\text{Alpha}=2.50$

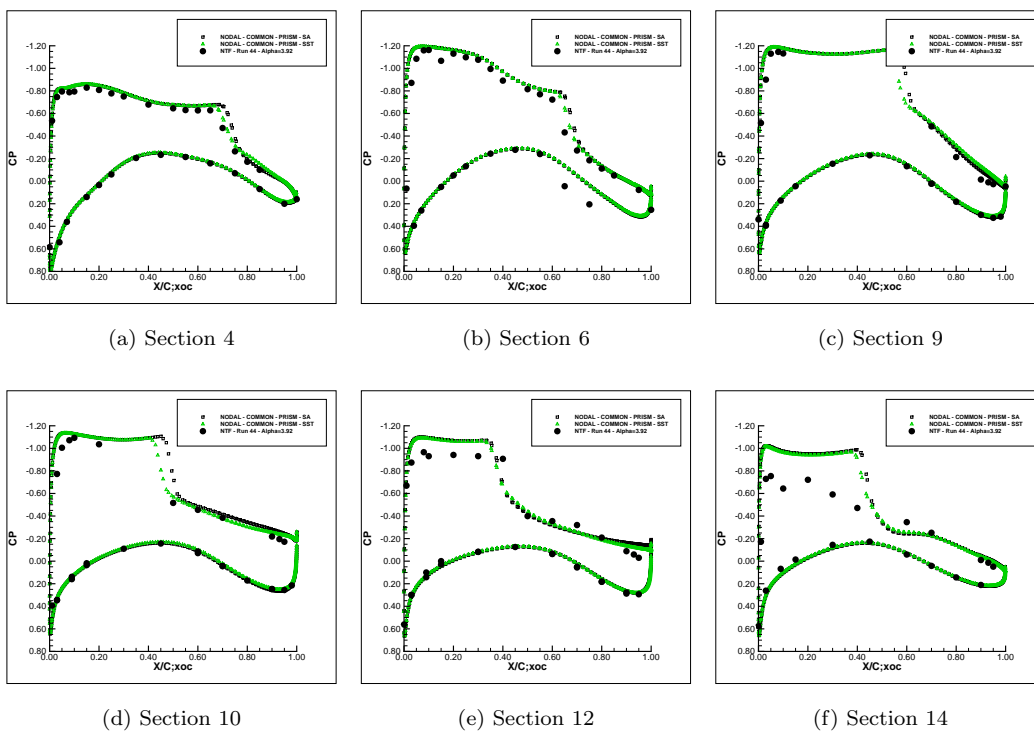


Figure 22. Pressure coefficient distributions,  $M=0.85$ ,  $Re=5$  millions and  $\text{Alpha}=4.00$

## IV. Conclusion

The commercial CFD software CFD++ was used to simulate the flow over the CRM model using several grids and different turbulence models. A total of 6 different set of grids were used, 3 provided by the DPW-5 Committee and 4 generated by EMBRAER. It was observed that the set of grids provided by the DPW-5 committee reached grid convergence sooner and showed better agreement with the experimental values for total drag. These grids were very similar in relation to each other because they were all generated based on the CommonHex grid. Besides the original CommonHex grid, it was created a triangular base prism grid (CommonPrism) and a tetrahedra grid (CommonHybrid). Even though the CommonPrism and CommonHybrid are unstructure grids, they present faces aligned to the flow direction because they are generated from the CommonHex grid.

The simulations using the grids generated at EMBRAER presented difficulties to converge the pressure drag. The simulations also presented difficulties to converge the fuselage and wing contributions. Further improvements in the surface grid allowed a better convergence of fuselage drag. Surface grid and volume grid improvements were not enough to improve wing drag convergence. This fact may suggest that grid resolution alone is not enough to reduce the wing drag dependence on the grid. This is probably due to the presence of the shock wave and the fact that the grids generated at EMBRAER are truly unstructured grids made of triangular prisms and tetrahedra. They do not have the same regularity presented by the Common set of grids provided by DPW-5.

The buffeting study also highlighted the flow solution dependence on the grids. The dependence on the grid is very high when strong shocks start to form over the wing and significant flow separation occurs. Even flow solutions using the regularly spaced Common grids from DPW-5 presented significant variation on the CL x Alpha, CM x CL and CD x CL curves. It could be observed that the CommonHex and CommonPrism grids are in closer agreement with each other and that the CommonHybrid grid stands apart. This is probably due to the numerical difficulties generated by using grids with tetrahedra, which tend to be more dissipative.

The results of comparisons using different turbulence models indicate small variations of flow quantities when the flow is attached with mild shocks ( $M=0.85$ ,  $CL=0.50$ ). In the buffeting study, the change of turbulence model generated spread similar to the observed when using different sets of grids. It was observed that the simulations using the SA model consistently predict a more aft shock wave position than the SST model.

## Acknowledgments

The authors are indebted to the AIAA DPW-5 Committee for the fruitful discussions about drag prediction and the application of CFD in an engineering environment.

## References

- <sup>1</sup>Hirsch, C., "Numerical Computation of Internal and External Flows", Vol. 2, 1990.
- <sup>2</sup>Levy, D. W., Wahls, R. A., Zickuhr, T., Vassberg, J., Agrawal, S., Pirzadeh, S., Hensch, M. J., "Summary of data from the first AIAA CFD Drag Prediction Workshop", AIAA-2002-841, 40th AIAA Aerospace Sciences Meeting and Exhibit, Reno, NV, Jan. 14-17, 2002
- <sup>3</sup>Laffin, K. Brodersen, O., Rakowitz, M., Vassberg, J., Wahls, R., Morrison J., Tinoco, E., Godard J.L., "Summary of Data from the Second AIAA CFD Drag Prediction Workshop", AIAA-2004-555, 42nd AIAA Aerospace Sciences Meeting and Exhibit, Reno, Nevada, Jan. 5-8, 2004
- <sup>4</sup>Vassberg, J., Tinoco, E., Mani, M., Brodersen, O., Eisfeld, B., Wahls, R., Morrison, J., Zickuhr, T., Laffin, K., Mavriplis, D., "Summary of the Third AIAA CFD Drag Prediction Workshop", AIAA-2007-260, 45th AIAA Aerospace Sciences Meeting and Exhibit, Reno, Nevada, Jan. 8-11, 2007
- <sup>5</sup>Vassberg, J., Tinoco, E., Mani, M., Rider, B., Zickuhr, T., Levy, D., Brodersen, O., Eisfeld, B., Crippa, S., Wahls, R., Morrison, J. Mavriplis, D., Murayama, M., "Summary of the Fourth AIAA CFD Drag Prediction Workshop", AIAA-2010-4547, 28th AIAA Applied Aerodynamics Conference, Chicago, Illinois, June 28-1, 2010
- <sup>6</sup>Vassberg, J., Dehaan, M., Rivers, M., Wahls, R., "Development of a Common Research Model for Applied CFD Validation Studies", AIAA-2008-6919, 26th AIAA Applied Aerodynamics Conference, Honolulu, Hawaii, Aug. 18-21, 2008
- <sup>7</sup>Vassberg, J., "A Unified Baseline Grid about the Common Research Model Wing/Body for the Fifth AIAA CFD Drag Prediction Workshop (Invited)", AIAA-2011-3508, 29th AIAA Applied Aerodynamics Conference, Honolulu, Hawaii, June 27-30, 2011
- <sup>8</sup>Rivers, M., Jacobs, A.D., "Experimental Investigations of the NASA Common Research Model in the NASA Langley

National Transonic Facility and NASA Ames 11-Ft Transonic Wind Tunnel (Invited)", AIAA-2011-1126, 49th AIAA Aerospace Sciences Meeting including the New Horizons Forum and Aerospace Exposition, Orlando, Florida, Jan. 4-7, 2011

<sup>9</sup>Peroomian, O., and Chakravarthy, S., "A 'Grid-Transparent' Methodology for CFD," AIAA Paper No. 97-0724, Reno 1997.

<sup>10</sup>Chakravarthy, S., Goldberg, U., Peroomian, O. and Sekar, B. "Some Algorithmic Issues in Viscous Flows Explored using a Unified-Grid CFD Methodology," 13th AIAA CFD Conference, Snowmass, June 1997.

<sup>11</sup>Chakravarthy, S., Peroomian, O. and Sekar, B., "Some Internal Flow Applications of a Unified-Grid CFD Methodology," AIAA Paper No. 96-2024, Florida 1996.

<sup>12</sup>Goldberg U, "Turbulence Closure with a Topography-parameter-free Single Equation Model, International Journal of Computational Fluid Dynamics, Vol. 17(1), pp. 27-38, 2003

<sup>13</sup>Spalart, P. R. and Allmaras, S. R., "A One-Equation Turbulence Model for Aerodynamic Flows," Recherche Aerospatale, No. 1, 1994, pp. 5-21

<sup>14</sup>Spalart, P. R., "Trends in Turbulence Treatments," AIAA 2000-2306, June 2000.

<sup>15</sup>Spalart, P. R. and Rumsey, C. L., "Effective Inflow Conditions for Turbulence Models in Aerodynamic Calculations," AIAA Journal, Vol. 45, No. 10, 2007, pp. 2544-2553.

<sup>16</sup>Menter, F. R., "Two-Equation Eddy-Viscosity Turbulence Models for Engineering Applications," AIAA Journal, Vol. 32, No. 8, August 1994, pp. 1598-1605.

<sup>17</sup>Rivers, M., Hunter, C., "Further Investigation of the Support System Effects and Wing Twist on the NASA Common Research Model", AIAA-2012-3209, 30th AIAA Applied Aerodynamics Conference, New Orleans, Louisiana, June 25-28, 2012